Hindawi
Geofluids
Volume 2021, Article ID 8846132, 7 pages
https://doi.org/10.1155/2021/8846132

Research Article

On the Imbibition Model for Oil-Water Replacement of Tight Sandstone Oil Reservoirs

Xiong Liu, Desheng Zhou, Le Yan, Shun Liu, and Yafei Liu

School of Petroleum Engineering, Xi'an Shiyou University, Xi'an, China

Correspondence should be addressed to Shun Liu; 53337220@qq.com

Received 13 May 2020; Accepted 28 April 2021; Published 24 May 2021

Academic Editor: Umberta Tinivella

A model suitable for evaluating a tight sandstone reservoir is established. The model includes two oil-water replacement modes: capillary force mode and osmotic pressure mode. The relationship between oil-water displacement rate and dimensionless time under different parameters is drawn considering the influence of capillary force, osmotic pressure, production pressure difference, and starting pressure gradient. Results indicate that the higher the relative permeability of the water phase, the lower the relative permeability of the oil phase, the smaller the oil-water viscosity ratio, and the higher the oil-water replacement rate. The relative permeability of the water phase also affects the infiltration stabilization time. Low salinity fracturing fluid infiltration helps to improve the oil-water replacement rate.

1. Introduction

"Fracture network fracturing and oil-water infiltration and replacement" is a new attempt for effective development of tight sandstone reservoirs. The tight reservoir and physical properties provide great conditions for fluid imbibition and replacement. Fracturing fluid is not only the carrier of carrying sand to make fracture but also the tool of displacement. The widely recognized oil/water displacement modes of tight reservoirs include three main models: reverse imbibition replacement, replacement of infiltration, and absorption in the same direction and osmotic pressure replacement. The first two models are fluid imbibition displacement under capillary force, and the latter is based on the displacement caused by osmotic pressure difference caused by ionic concentration difference. Many scholars have done a lot of research in this area. In terms of imbibition and replacement, most laboratory experiments show that the imbibition process is the infiltration of the injected water into the pore channel under capillary force, driving the oil and gas resources away from the adjacent macropores, so as to realize imbibition replacement [1–4]. The scholars Oen et al. [5], Babadagli and Ershaghi [6], Shabir et al. [7], and the ET (Tayfun) (2015) have studied the imbibition and displacement between cracks and matrix in fractured reservoirs and studied the imbibition characteristics of shale formations. Bertoncello et al. [8] based on imbibition to study the self-priming of single-well fracturing during the early stage of unconventional reservoirs. In terms of osmotic pressure replacement, Mitchell et al. [9], Kurtoglu [10], van Oort et al. [11], Xu et al. [12], [13], and ET (2016) et al. have mainly studied the characteristics of osmotic pressure and oil and water displacement in shale reservoirs and have studied in detail. Mirzaei et al. [14], Kathel and Mohanty [15], and Chahardowli et al. [16] studied that low salinity brine is an effective way to improve the recovery of fractured tight sandstone reservoirs.

Research on factors affecting oil-water imbibition and displacement in tight reservoirs: scholars Mirzaei et al. [14] based on CT scanning experimental methods, the factors affecting the permeability of fractured cores of oil wetting fracture are analyzed and studied. It is considered that wetting and viscosity are the main factors affecting the imbibition effect of oil wetting fractured cores. The research shows that the methods of increasing oil recovery in fractured oil reservoirs include steam injection, low salinity brine, and surfactant. Kathel and Mohanty [15] consider that the main controlling factors affecting the recovery of tight reservoirs are as follows: wettability > salt concentration > residual oil saturation; and

Liang et al. [17] for Buchan tight reservoirs, the influence parameters of single-well productivity are analyzed by means of information analysis, grey correlation, and orthogonal experimental design. Besides fracture parameters, reservoir permeability, formation pressure, and viscosity of crude oil have great influence on the output of a single well. Lan et al. [18] explore the relationship between the imbibition and water loss of a tight sandstone reservoir and the soaking time. The results show that the change of clay content has no effect on imbibition. The larger the TOC content is, the lower the permeation capacity is. Habibi et al.'s [19] study shows that the imbibition position in the same rock core is random. Saline immersion can help to increase the close relationship between fluid and rock and affect the contact angle size. Chahardowli et al.'s [16] study shows that the application of brine to weak water wetting and mixed wetting core improves EOR, and the first oil recovery can reach 38-46% OIIP. Valluri et al.'s [20] study shows that the interaction between sodium and calcium saline water and ultralow density rocks helps to enhance the recovery of tight reservoirs. Qing et al. [21] study the Chang 8 reservoir in the Wu Qi area by means of geothermal nitrogen adsorption, high-pressure mercury injection, Amott method, and imbibition NMR. The influencing factors are reservoir quality, maximum pore throat radius, specific surface area, and relative wetting index.

In summary, the mechanism of oil-water displacement in tight sandstone reservoirs is not clear enough. Most of them are based on laboratory experiments and analysis. Few literatures consider two models of displacement and replacement under the action of capillary force.

2. Displacement Mechanism

Tight sandstone reservoirs cannot form natural industrial productivity and need horizontal-well fracturing for reservoir reconstruction. Fracturing fluid can not only break the rock to communicate with fractures and form a complex fracture network but also replace the oil phase with a matrix to increase the output of a single well. The widely recognized mechanism of oil and water displacement in tight reservoirs includes capillary imbibition and displacement under osmotic pressure. As shown in Figure 1, assuming that reservoirs are hydrophilic, the water phase enters the throat under capillary force, the displacement of oil phase from the other end of the pore throat, the smaller the throat, the greater the capillary force, the more oil and water displacement. The pore throat of a tight sandstone reservoir is mostly concentrated in 0.1-1 μm, so capillary force is more significant. Figure 2 shows the osmotic pressure mechanism. The low permeability solution on the left side of the semipermeable membrane and the high salinity solution on the right side, because of the osmotic pressure generated by the ion concentration difference on both sides, the water molecules in the low salinity solution of the left pipeline are under osmotic pressure. Through the semipermeable membrane into the right pipe, until the force is balanced again, the clay minerals in the tight sandstone reservoir contain 5%-10% oil. Two sides of the clay will produce double ionosphere, which has the function of semipermeable membrane. When the fracturing fluid and the formation water have poor mineralization, they will form osmotic pressure on both sides of the clay mineral, if the fracturing fluid salinity is relatively low. Then, the water molecules in the fracturing fluid penetrate the clay minerals into the reservoir, and the displacement of the oil phase is expelled from the other port. This is also the reason for the low salinity water drive to enhance the oil recovery.

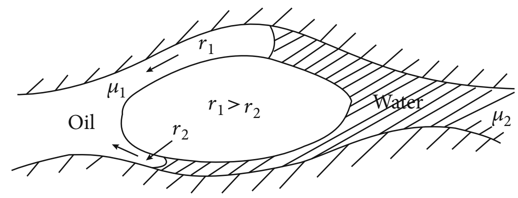

Figure 1: Oil and water displacement under capillary force.

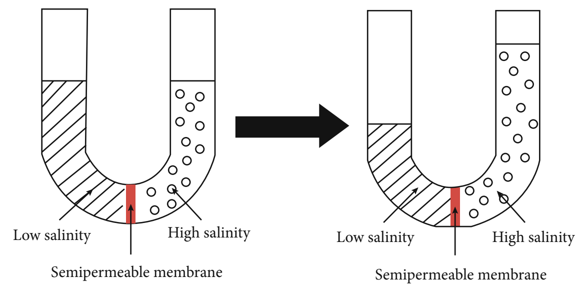

Figure 2: Oil-water displacement under osmotic pressure.

Figures 3 and 4 show the core gravity imbibition experimental device and the experimental data of tight sandstone cores with capillary force and osmotic pressure, respectively. The experimental cores are taken from the Chang 7 group of tight sandstone reservoirs in Changqing Oilfield (China). The permeability of the core is $0.084 \times 10^{-3}\ \mu m^2$, the porosity is 7.39%, and the clay mineral content is 6.69%. The experimental process is as follows: (1) using core cutting machine, core drilling machine, and core grinding machine, the cores obtained from the field are made into standard rock samples with diameters of 2.5 cm and 4-5 cm in length. (2) The standard rock samples are washed and dried to constant weight, core weight is recorded, porosity and permeability are measured, and so on. (3) Saturate distilled water, then displace the saturated simulated oil, and leave it in the simulated oil for a period of time. (4) Wipe off the surface oil slick, and carry out the experiment by using the weighing method core imbibition experiment device shown in Figure 3; (5) record and process the experimental data; (6) after the experiment is finished, remove the core, reprocess steps (2) and (3), and proceed to the next group of experiments to make the experimental results have higher credibility.

A total of 3 sets of comparative experiments were carried out. As shown in Figure 4, the percolating solution was distilled water, 15000 mg/L mineralized solution (according to the formation water ion configuration), and 45000 mg/L mineralized solution, because the degree of osmotic fluid mineralization is larger than that of the core water phase, resulting in the opposite direction of the osmotic pressure

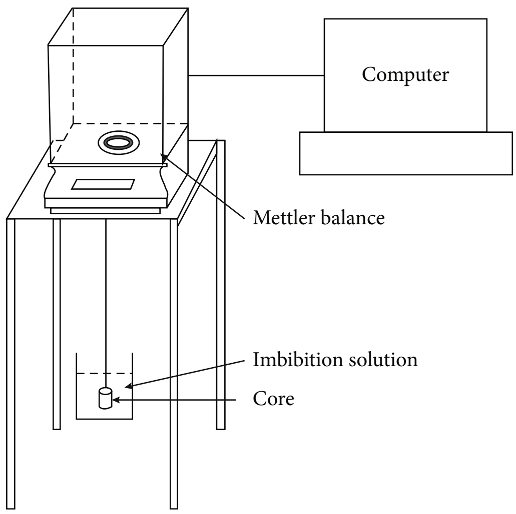

FIGURE 3: Weighting core imbibition experimental device.

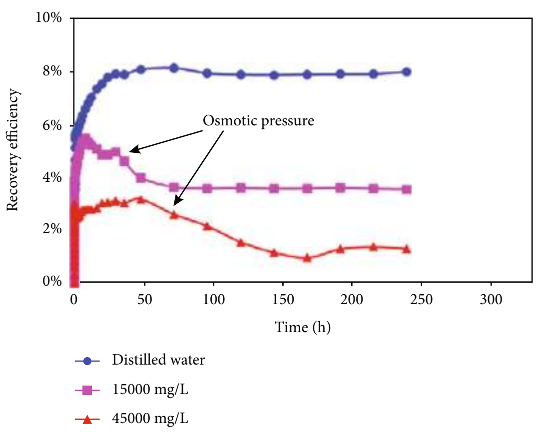

FIGURE 4: Imbibition test data of tight sandstone core considering capillary force and osmotic pressure.

direction and capillary force, which is convenient for experimental observation. From the comparison of the 3 curves, we can see that osmotic pressure is more obvious, and the downward section of the imbibition curve with downward osmotic pressure will have a downward trend. The greater the osmotic pressure, the greater the downward trend. This is because the capillary force in the early stage of osmosis is much larger than that of osmotic pressure, and the overall performance of the curve is rising rapidly. The overall force of the fluid tends to be balanced, the capillary force displacement reaches the limit, and the osmotic pressure displacement characteristics are revealed. The experimental results show that there are two modes of oil-water replacement in tight sandstone reservoirs: oil-water infiltration and replacement under capillary pressure and displacement under osmotic pressure.

3. Model Establishment

After fracturing, the tight sandstone oil reservoir is fractured by horizontal wells. The oil phase flows from the matrix to the fracture network and then converges to the bottom of the well. The oil and water displacement occurs mainly in the flow network of the fracture network under the capillary force and osmotic pressure. The displacement of fluid can be regarded as a one-dimensional seepage process perpendicular to the fracture surface. As shown in Figure 5, a one-dimensional oil and water imbibition displacement model is constructed. The assumptions of the model include the following: (1) homogeneous and isotropic reservoir, rock and fluid slightly compressible; (2) oil-water two-phase isothermal percolation; (3) considering the effects of production pressure difference, capillary force, osmotic pressure, gravity, and starting pressure gradient; (4) salts only dissolve in the water; and (5) no physical and chemical reaction.

As shown in Figure 5, the left side is the fracture surface, the position for fluid replacement, and the right side is the fluid displacement limit distance, and the approximate closed end. Take the gravity effect into account, the equation of motion of the water phase and oil phase can be expressed as

$$v_{\mathrm{w}} = -\frac{kk_{\mathrm{rw}}}{\mu_{\mathrm{w}}}\left(\frac{\partial p_{\mathrm{w}}}{\partial z} + \rho_{\mathrm{w}} g \sin\theta\right), \tag{1}$$

$$v_{\mathrm{o}} = -\frac{kk_{\mathrm{ro}}}{\mu_{\mathrm{o}}}\left(\frac{\partial p_{\mathrm{o}}}{\partial z} + \rho_{\mathrm{o}} g \sin\theta\right). \tag{2}$$

Considering the microcompressibility of rock and fluid, the seepage velocity of water-phase and oil-phase fluid is satisfied:

$$v_{\mathrm{o}} + v_{\mathrm{w}} = 0. \tag{3}$$

The saturation equation is as follows:

$$\varphi\frac{\partial S_{\mathrm{w}}}{\partial t} + \frac{\partial v_{\mathrm{w}}}{\partial z} = 0. \tag{4}$$

The relative permeability curve is characterized by the Corey equation:

$$\begin{cases} k_{rw} = k_{\mathrm{rw}}^{*} S^{a}, \\ k_{\mathrm{ro}} = k_{\mathrm{ro}}^{*}(1-S)^{b}, \\ S = \dfrac{S_{\mathrm{w}} - S_{wi}}{1 - S_{\mathrm{or}} - S_{\mathrm{wi}}}. \end{cases} \tag{5}$$

Capillary pressure is expressed by the J function:

$$P_{\mathrm{c}} = J(S)\sigma\sqrt{\frac{\varphi}{k}}. \tag{6}$$

Formula: $J(S) = eS^{d}$.

Scholars Marine and Fritz [22] describe the osmotic pressure formula:

$$\Pi = \frac{RT_{c}}{V}\ln\left(\frac{a_{I}}{a_{\mathrm{II}}}\right). \tag{7}$$

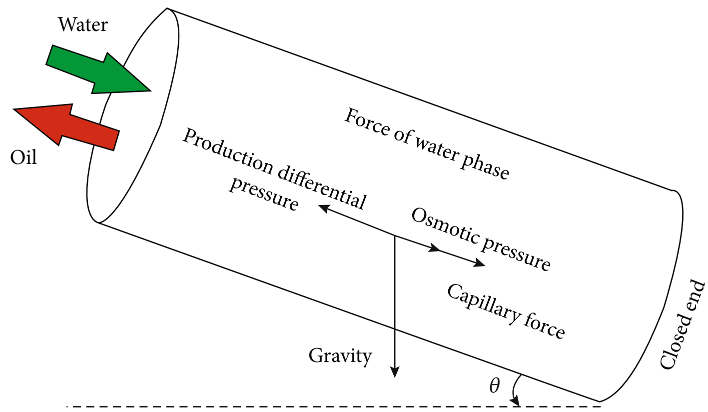

Figure 5: Oil-water percolation displacement model.

The reservoir is dense, and the flow of fluid in the reservoir follows the low-velocity non-Darcy law. Considering the effects of osmotic pressure, production pressure difference, and starting pressure gradient, comprehensive formula (1)–formula (7) can be rewritten as

$$\varphi \frac{\partial S_w}{\partial t} + \frac{\partial}{\partial z}\left[\frac{k k_{rw} k_{ro}}{k_{ro}\mu_w + k_{rw}\mu_o}\left(\frac{\partial p_c}{\partial z} - \Delta\rho g \sin\theta - \frac{\partial \Pi}{\partial z} + \Delta P + G\right)\right] = 0. \tag{8}$$

Formula: $\Delta\rho = \rho_w - \rho_o$.
Dimensionless transformation:

$$\begin{cases} Z = \dfrac{z}{L}, \\ T = \dfrac{\sigma}{\mu_w L^2}\sqrt{\dfrac{k}{\varphi}}t. \end{cases} \tag{9}$$

Dimensionless processing, formula (8) transforms the expression:

$$\frac{\partial S}{\partial T} + A\frac{1}{\partial Z}\left[f(S)\begin{pmatrix} \dfrac{\partial J(S)}{\partial S}\dfrac{\partial S}{\partial Z} - \dfrac{L}{\sigma}\sqrt{\dfrac{k}{\varphi}}\Delta\rho g \sin\theta \\ -\dfrac{1}{\sigma}\sqrt{\dfrac{k}{\varphi}}\left(\dfrac{\partial \Pi}{\partial Z} - L\Delta P - LG\right)\end{pmatrix}\right] = 0. \tag{10}$$

Formula:

$$\begin{aligned} A &= \frac{\mu_w}{1 - S_{or} - S_{wi}}, \\ f(S) &= \frac{k_{rw}^* S^a k_{ro}^* (1-S)^b}{k_{rw}^* S^a \mu_o + k_{ro}^* (1-S)^b \mu_w}. \end{aligned} \tag{11}$$

The discretization equations are as follows:

$$\begin{aligned} &-A\frac{\nabla T}{\nabla Z^2} f\left(S_{i-1/2}^{m+1}\right)\frac{\partial J(S)}{\partial S} S_{i-1}^{m+1}\left[1 + A\frac{\nabla T}{\nabla Z^2}\left(f\left(S_{i+1/2}^{m+1}\right)\frac{\partial J(S)}{\partial S}\right.\right. \\ &\qquad \left.\left. + f\left(S_{i-1/2}^{m+1}\right)\frac{\partial J(S)}{\partial S}\right)\right]S_i^{m+1} - A\frac{\nabla T}{\nabla Z^2} f\left(S_{i+1/2}^{m+1}\right)\frac{\partial J(S)}{\partial S} S_{i+1}^{m+1} \\ &\quad = S_i^m + A\frac{\nabla T}{\nabla Z}\left[f\left(S_{i+1/2}^{m+1}\right) - f\left(S_{i-1/2}^{m+1}\right)\right]\frac{L}{\sigma}\sqrt{\frac{K}{\varphi}}\Delta\rho g \sin\theta \\ &\qquad + \frac{A}{\sigma}\sqrt{\frac{k}{\varphi}}\left\{\frac{\Delta T}{\Delta Z}\left[\left(\Pi_{i+1}^m - \Pi_i^m\right) f\left(S_{i+1/2}^m\right)\right.\right. \\ &\qquad \left.\left. - \left(\Pi_i^m - \Pi_{i-1}^m\right) f\left(S_{i-1/2}^m\right)\right] - L\Delta P - LG\right\}. \end{aligned} \tag{12}$$

It is assumed that the mineralization degree of fracturing fluid (water phase) is constant. Every time step needs to update the mineralization of each grid in the reservoir. If the grid size is uniform, the calculation formula of the corresponding mineralization degree of each grid is as follows:

$$c_i^{m+1} = \frac{c_{i-1}^m\left(S_i^{m+1} - S_i^m + \sum_{i+1}^N\left(S_j^{m+1} - S_j^m\right)\right) + c_i^m\left(S_i^m + S_c - \sum_{i+1}^N\left(S_j^{m+1} - S_j^m\right)\right)}{S_i^{m+1} + S_c}. \tag{13}$$

By means of formula (12), the dimensionless saturation distribution along the path can be obtained, and the formula of oil-water displacement rate can be obtained by integrating the dimensionless saturation:

$$\eta(T) = \frac{\int_0^L S(Z,T)\,dZ}{L}. \tag{14}$$

4. Sensitivity Analysis

The basic model parameters of sensitivity analysis are $k = 0.02 \times 10^{-3}\,\mu\text{m}^2$, $\varphi = 0.06$, $k_{rw}^* = 0.2$, $k_{ro}^* = 1.0$, $u_o/u_w = 0.5$, $u_w = 1.0$, $a = 2.65$, $b = 3.54$, $d = 4.8088$, $e = 0.0062$, $\theta = 0°$, $S_{wi} = 39.61\%$, $S_{or} = 30.83\%$, $N = 41$, compressive fracture fluid mineralization of 0 mg/L and remain unchanged, and water-phase initial mineralization of 25000 mg/L in a

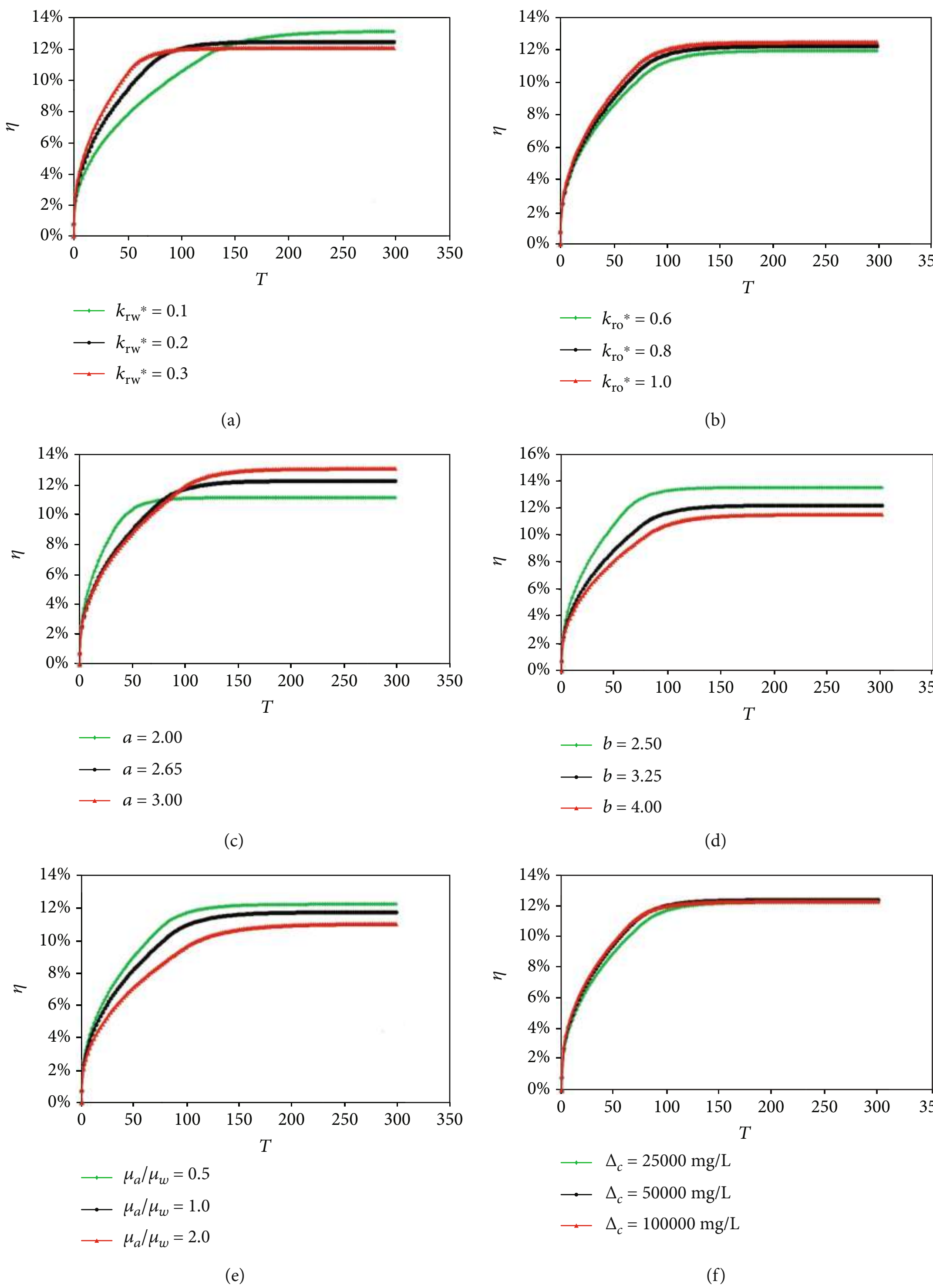

FIGURE 6: (a) When $k_{rw}^* = 0.1, 0.2$, and 0.3, the relationship between oil-water displacement rate and dimensionless time; (b) when $k_{ro}^* = 0.6, 0.8$, and 1.0, the relationship between oil-water displacement rate and dimensionless time; (c) when $a = 2.00, 2.65$, and 3.00, the relationship between oil-water displacement rate and dimensionless time; (d) when $b = 2.50, 3.25$, and 4.00, the relationship between oil-water displacement rate and dimensionless time; (e) when $u_o/u_w = 0.5, 1.0$, and 2.0, the relationship between oil-water displacement rate and dimensionless time; (f) when $\Delta c = 25000$ mg/L, 50000 mg/L, and 100000 mg/L, the relationship between oil-water displacement rate and dimensionless time.

reservoir. The relation curve between oil-water displacement rate and dimensionless time is drawn (Figure 6).

Figure 6(a) shows the relationship between oil-water replacement rate and dimensionless time when the maximum water-phase relative permeability value is 01, 0.2, and 0.3. From the curve comparison, it can be seen that the larger the maximum water-phase relative permeability value, the shorter the oil-water replacement time reaches the stable state, the lower the oil-water replacement rate; Figure 6(b) shows the maximum oil-phase relative permeability value is 0.6, 0.8, and 1. The relationship between oil-water displacement rate and nondimensional time is shown. It can be seen from the figure that the maximum relative permeability of oil phase has little influence on the oil-water replacement process. The larger the maximum relative permeability of oil phase is, the higher the oil-water replacement rate is. Figure 6(c) shows the relationship between oil-water displacement rate and dimensionless time when the water phase coefficient is 2.00, 2.65, and 3.00. From the diagram, it can be seen that the larger the water-phase coefficient is, the larger the oil-water displacement rate is, and the longer the time to reach the stable imbibition is. Figure 6(d) shows the relationship between oil-water displacement rate and dimensionless time when the oil-phase coefficient is 2.50, 3.25, and 4.00. It can be seen from the figure that the oil-phase coefficient has a little effect on the seepage and absorption stability time but has an obvious effect on the oil-water displacement rate. The smaller the oil-phase coefficient is, the greater the oil-water displacement rate is; Figure 6(e) shows the relationship between oil-water displacement rate and dimensionless time when the oil-water viscosity ratio is 0.5, 1.0, and 2.0. It can be seen from the curve that the smaller the oil-water viscosity ratio is, the higher the oil-water displacement rate is; Figure 6(f) shows the relationship between oil-water displacement rate and dimensionless time when the salinity difference is 25000 mg/L, 50000 mg/L, and 100000 mg/L. It is not difficult to see that the salinity difference has a certain impact on the infiltration and absorption process, but the impact is small.

5. Conclusions

A model for evaluating the permeability of tight sandstone reservoirs with capillary force and osmotic pressure is established. The model takes into account the influence of capillary force, osmotic pressure, production pressure difference, and starting pressure gradient on the process of oil-water permeation and displacement.

(1) The main control factors affecting the process include the relative permeability of water phase, the relative permeability of oil phase, the oil-water viscosity ratio, the higher the relative permeability of water phase, the lower the relative permeability of oil phase, the smaller the oil-water viscosity ratio, and the higher the oil-water displacement ratio

(2) The relative permeability of the water phase affects the infiltration stabilization time, and the larger the relative permeability of the water phase, the longer the infiltration stabilization time

(3) Low salinity fracturing fluid infiltration can improve the oil-water displacement rate, but the effect is small

Nomenclature

a: The water-phase coefficient is dimensionless
a_{I}: Low salinity water molar fraction (%)
a_{II}: High salinity water molar fraction (%)
b: The oil-phase coefficient is dimensionless
B: Coefficient, dimensionless
c: Mineralization (mg/L)
Δc: Salinity difference (mg/L)
d: J function exponential coefficient, dimensionless
e: J function coefficients, dimensionless
g: Acceleration of gravity (m/s^2)
G: Starts the pressure gradient (MPa/m)
i: Grid i
j: Grid j
$J(S)$: J function
k: Absolute permeability of reservoir ($1 \times 10^{-3}\ \mu\mathrm{m}^2$)
k_{rw}: The relative permeability of water phase is dimensionless
k_{ro}: The relative permeability of oil phase is dimensionless
k^*_{rw}: The maximum relative permeability of water phase is dimensionless
k^*_{ro}: The maximum relative permeability of oil phase is dimensionless
L: Model length (m)
m: Time step (m)
N: Discrete grid number, dimensionless
p_{w}: Water pressure (MPa)
p_{o}: Oil-phase pressure (MPa)
p_{c}: Capillary force (MPa)
R: The R constant is equal to 0.00831 MPa·L/(K·Mol)
S: Standardized water saturation is dimensionless
S_{c}: Standardized bound water saturation, dimensionless
S_{wi}: Irreducible water saturation is dimensionless
S_{or}: Residual oil saturation is dimensionless
S_{w}: The water saturation is dimensionless
T: Dimensionless time and dimensionless
t: Time (s)
μ_w: Water viscosity (mPa·s)
μ_{o}: Viscosity of oil phase (mPa·s)
v_{w}: Velocity of seepage in water phase (m/d)
v_{o}: Velocity of oil-phase seepage (m/d)
V: Water molar volume (0.018 L/mol)
z: Coordinate position (m)
Z: Dimensionless coordinate position, dimensionless
ρ_{w}: Water density (kg/m^3)
ρ_{o}: Oil-phase density (kg/m^3)
σ: Interfacial tension (mN/m)
φ: Porosity, decimal fraction
θ: Horizontal angle
η: Oil water replacement rate, decimal fraction

Π: Osmotic pressure (MPa)
T_c: Temperature (Kelvin)
ΔP: Production pressure difference (MPa).

Data Availability

Raw data and derived data supporting the findings of this study are available from the corresponding author Xiong Liu (Email: lx06106232@163.com) on request.

Conflicts of Interest

The authors declare that they have no conflicts of interest.

Acknowledgments

Xiong Liu would like to acknowledge the Chinese National Natural Science Foundation (No. 51804257) for providing research funding. Desheng Zhou would like to acknowledge the Chinese National Natural Science Foundation (No. 51934005 and No. 51874242) for providing research funding. Shun Liu would like to acknowledge the Natural Science Basic Research Program of Shaanxi (Program No. 2019JQ-403) for providing research funding.

References

[1] B. Roychaudhuri, J. Xu, T. T. Tsotsis, and K. Jessen, "Forced and spontaneous imbibition experiments for quantifying surfactant efficiency in tight shales," in *SPE 169500, SPE Western north American and Rocky Mountain and Rocky Mountain joint regional meeting held in*, pp. 16–18, Denver, Colorado, USA, 2014.

[2] K. Makhanov, H. Dehghanpour, and E. Kuru, "An experimental study of spontaneous imbibition in Horn River Shales," in *SPE 162650, SPE Canadian unconventional resources conference held in*, Calgary, Alverta, Canada, 2012.

[3] L. Shuai, D. Yunhong, M. Di et al., "Volume transformation experiment and multi-scale simulation of," *Oil drilling technology considering imbibition and displacement*, vol. 38, no. 5, pp. 678–683, 2016.

[4] P. Yu, X. Wang, and P. Ling, "Static reservoir imbibition experiment," *Daqing petroleum geology and development*, vol. 35, no. 6, pp. 159–163, 2016.

[5] P. M. Oen, M. Engell-Jensen, and A. A. Barendregt, "Skjold field, Danish north sea: early evaluations of oil recovery through water imbibition in a fractured reservoir," *SPE Reservoir Engineering*, vol. 3, no. 1, pp. 17–22, 1988.

[6] T. Babadagli and I. Ershaghi, "Imbibition assisted two-phase flow in natural fractures," in *SPE 24044, Western regional meeting*, Bakersfield, CA, 1992.

[7] S. Al-Lawati and S. Saleh, "Oil recovery in fractured oil reservoirs by low IFT imbibition process," in *SPE 36688, SPE annual technical conference and exhibition held in*, pp. 6–9, Denver, Colorado, USA, October 1996.

[8] A. Bertoncello, J. Wallace, H. Corp, C. Blyton, M. Honarpour, C. S. Kabir et al., "Imbibition and water blockage in unconventional reservoirs: well management implications during flowback and early production," in *SPE 167698, SPE/EAGE European unconventional conference and exhibition held in*, pp. 25–27, Vienna, Austria, 2014.

[9] J. K. Mitchell and K. Soga, *Fundamentals of Soil Behavior*, John Wiley & Sons, Hoboken, N.J, 3rd edition, 2005.

[10] B. Kurtoglu*Integrated Reservoir Characterization and Modeling in Support of Enhanced Oil Recovery for Bakken*, Colorado School of Mines, USA, 2013.

[11] E. van Oort, M. Ahmad, R. Spencer, and N. Legacy, "ROP enhancement in shales through osmotic processes," in *SPE 173138, SPE/IADC Drilling conference and exhibition held in*, London, U.K, 2015.

[12] J. Xu, K. Wu, S. Yang et al., "Real gas transport in tapered noncircular nanopores of shale rocks," *AIChE Journal*, vol. 63, no. 7, pp. 3224–3242, 2017.

[13] J. Xu, K. Wu, R. Li et al., "Real gas transport in shale matrix with fractal structures," *Fuel*, vol. 219, pp. 353–363, 2018.

[14] M. Mirzaei, D. A. Dicarlo, and G. A. Pope, "Visualization and analysis of surfactant imbibition into oil-wet fractured core," in *SPE 166129, SPE Annual Technical Conference and Exhibition*, New Orleans, 2013.

[15] P. Kathel and K. K. Mohanty, "EOR in tight oil reservoirs through wettability alteration," in *SPE 166281, SPE Annual Technical Conference and Exhibition*, New Orleans, 2013.

[16] M. Chahardowli, R. Farajzadeh, S. K. Masalmeh, H. Mahani, and H. Bruining, "A novel enhanced oil recovery technology using dimethyl ether/brine: spontaneous imbibition in sandstone and carbonate rocks," in *SPE 181340, SPE annual technical conference and exhibition held in*, pp. 26–28, Dubai, UAE, September 2016.

[17] L. Tao, C. Y. Wen, G. Xiaofei et al., "The order of influence degree of single well productivity parameter in tight oil reservoir," *Petroleum exploration and development*, vol. 40, no. 3, pp. 357–362, 2013.

[18] Q. Lan, E. Ghanbari, H. Dehghanpour, and R. Hawkes, "Water loss versus soaking time: spontaneous imbibition in tight rocks," in *SPE 167713, SPE/EAGE European unconventional conference and exhibition held in*, Vienna, Austria, 2014.

[19] A. Habibi, M. Binazadeh, H. Dehghanpour, D. Bryan, and G. Uswak, "Advances in understanding wettability of tight oil formations," in *SPE 175157, SPE Annual Technical Conference and Exhibition Held in Houston*, Texas, USA, 2015.

[20] M. K. Valluri, J. O. Alvarez, and D. S. Schechter, "Study of the rock/fluid interactions of sodium and calcium brines with ultra-tight rock surfaces and their impact on improving oil recovery by spontaneous imbibition," in *SPE 180274, SPE Low Perm Symposium Held in*, Denver, Colorado, USA, 2016.

[21] W. Qing, L. Zhiping, X. Wang et al., "Osmotic mechanism and influencing factors of fractured tight sandstone reservoirs: taking Chang 8 reservoir in Wuqi area of Ordos Basin as an example," *Oil and gas geology and recovery*, vol. 23, no. 4, pp. 102–107, 2016.

[22] I. W. Marine and S. J. Fritz, "Osmotic model to explain anomalous hydraulic heads," *Water Resources Research*, vol. 17, no. 1, pp. 73–82, 1981.